journal

J. Am. Ceram. Soc., **89** [7] 2096–2104 (2006)
DOI: 10.1111/j.1551-2916.2006.01067.x

Kinetic Effects on Hydroxyapatite Whiskers Synthesized by the Chelate Decomposition Method

Ryan K. Roeder,*,† Gabriel L. Converse, Huijie Leng, and Weimin Yue

Department of Aerospace and Mechanical Engineering, University of Notre Dame, Notre Dame, Indiana 46556

Hydroxyapatite (HA) whiskers have been synthesized using a number of chemical solution methods, including the chelate decomposition method. Numerous previous studies have investigated the effects of the reagents, reagent concentrations, solution pH, and reaction temperature on HA whisker morphology and composition. However, purely kinetic effects, such as the reaction heating and stirring rates, have not been rigorously investigated and are rarely reported in the literature. Therefore, the objective of this study was to investigate kinetic effects on the morphology of HA whiskers synthesized using the chelate decomposition method. In order to study the kinetic effects on the morphology of HA whiskers, three experimental parameters were varied independently: the reaction heating rate (0.36°–3.0°C/min), stirring rate (0–250 rpm), and temperature (80°–200°C). At all heating and stirring rates, precipitated whiskers were confirmed by XRD and FT-IR to comprise phase-pure, calcium-deficient HA (Ca/P = 1.57–1.62). The length and aspect ratio of HA whiskers increased with decreased heating rate, decreased stirring rate, and increased reaction temperature. The mean length and aspect ratio of HA whiskers increased approximately twofold with decreased heating rate over the range studied, following a power-law relationship. Therefore, the reaction heating rate is a key variable that can be used to tailor the morphology of HA whiskers and ought to be reported in the literature. The reaction heating rate and temperature had relatively little effect on the width of HA whiskers. However, the precipitate morphology was altered significantly from micro-scale whiskers to nano-scale plates with increased stirring rate. These results offered new insights and provided clarification regarding the reaction mechanism, which is discussed in detail.

I. Introduction

HYDROXYAPATITE (HA), $Ca_{10}(PO_4)_6(OH)_2$, is the closest synthetic equivalent to human bone mineral, which is a calcium and hydroxyl-deficient, carbonated apatite including other minor dopants such as magnesium and sodium.[1] Over 20 years of research has consistently shown that HA typically exhibits excellent biocompatibility, bioactivity, and, if porous, osteoconduction *in vivo*.[1–4] A limitation of HA ceramics in orthopedics has been inferior mechanical properties, most notably a low fracture resistance, which is exacerbated by the presence of porosity. Therefore, recent research has generally taken one of two directions: (1) toughening HA ceramics, or (2) reinforcing polymers with HA fillers. HA whiskers (short single crystal fibers) have been proposed to be advantageous for either toughening HA ceramics[5–7] or reinforcing polymers.[8,9] In reinforced polymers, the use of aligned HA whiskers instead of HA powder resulted in an improved stiffness, strength, toughness, and anisotropy more like that found in human cortical bone tissue.[9] Moreover, bone mineral crystals also exhibit an elongated *c*-axis (plate shaped) and a preferred orientation in directions of principal stress.[10,11]

The tendency of HA to form elongated crystals (whiskers, needles, or rods) was recognized in some of the earliest studies on the synthesis of HA.[12,13] HA whiskers have been synthesized by low-temperature chemical solution methods,[12–61] and high-temperature solid state,[62] or molten salt[63,64] reactions. Low-temperature chemical solution methods are the focus here, given that the application of reinforcing a polymer matrix does not require high-temperature stability and that these methods are more similar to biomineralization *in vivo*. An extensive literature review identified nearly 50 papers on the synthesis of HA whiskers using a variety of chemical solution methods.[12–61] In a general sense, all the methods could be described as "hydrothermal" processes. Therefore, methods were grouped more explicitly by the reaction mechanism as follows: chelate decomposition,[12–30] urea decomposition,[15,31–37] precipitation,[34,38–42] and hydrolysis of calcium phosphate precursors.[16,30,43–61]

The chelate decomposition method was first used in studies where large crystals were desired to study the crystallography of HA.[12,13] Yoshimura *et al.*[18] patented a process in 1991. Chelate decomposition includes all methods where a chelating agent, usually a carboxylic acid, is used to bind calcium ions in a homogeneous chemical solution. A wide range of carboxylic acids have been utilized; the most common have included acetic acid, lactic acid, citric acid, and ethylenediamine tetraacetic acid (EDTA). Upon heating the solution, or increasing the solution concentration by evaporation, the calcium carboxylate "decomposes" as the chemical equilibria shift and calcium is released into the phosphate-containing solution.[15,19–22] As the solution becomes supersaturated, calcium phosphate crystals nucleate and grow. The size and morphology of HA whiskers produced by chelate decomposition vary over a wide range at the micro-scale.

Urea decomposition takes advantage of an increase in solution pH caused by the slow hydrolysis of urea in aqueous solutions.[15,31] Acidic homogeneous solutions or suspensions containing a calcium phosphate precursor are prepared at pH$\approx$2–4 where HA is not stable. The incipient "decomposition" of urea gradually increases the solution pH above four, where HA is stable. HA crystals nucleate by dissolution and reprecipitation from calcium phosphate precursors and/or intermediate phases that precipitate.[32] HA whiskers produced by urea decomposition generally tend to have a greater size and aspect ratio than those produced by other methods.

Precipitation methods are those that do not utilize chemical additives to manipulate the chemical solution equilibria. Soluble reagents containing calcium and phosphate are used to precipitate HA crystals directly at temperatures less than 100°C. Note that one paper included here did investigate the effects of a wide range of additives using a two-solution mixing approach.[38] The additives were, however, added to the phosphate solution, not the calcium solution, and the solution pH was maintained at a fixed value independent of the additives. HA whiskers produced

T. Troczynski—contributing editor

Manuscript No. 20936. Received August 30, 2005; approved February 6, 2006.
This work was partially supported by the State of Indiana, 21st Century Research and Technology Fund.
*Member, American Ceramic Society.
†Author to whom correspondence should be addressed. e-mail: rroeder@nd.edu

by precipitation methods tend to be significantly smaller than those produced by other methods, typically on the nano-scale.

Hydrolysis of calcium phosphate precursors is governed by controlling the temperature or pH to induce the dissolution of a calcium phosphate precursor and reprecipitation of HA. Precursors have included amorphous calcium phosphate (ACP), anhydrous dicalcium phosphate (DCPA) or monetite, dicalcium phosphate dihydrate (DCPD) or brushite, α-tricalcium phosphate (α-TCP), monocalcium phosphate monohydrate (MCPM), calcium pyrophosphate, and calcium sulfate, which were treated at temperatures ranging from 37° to 450°C. Similar to precipitation, HA whiskers produced by these methods tend to be significantly smaller than those produced by other methods, typically on the nano-scale. However, in a noteworthy exception, large single-crystal HA whiskers, up to 1 cm long, were grown using sintered HA seeds and multiple heating zones to control heat transfer and convective flow in a pressure vessel.[52,53]

Overall, these studies have predominantly investigated the effects of the reagents, reagent concentrations, solution pH, and reaction temperature on HA whisker morphology and composition. Thus, chemical solution equilibria and resultant effects on whisker morphology have been examined, but purely kinetic effects, such as the reaction heating and stirring rates, have not. Early attempts in our laboratory to synthesize HA whiskers using chemical solution methods, in particular, the chelate decomposition method, suffered from an inability to replicate the whisker morphology (e.g., aspect ratio) reported by previous investigators. Further investigation revealed that the reaction heating rate is a critical parameter that is rarely reported in the literature. For example, of the nearly 50 papers cited above, only five reported a reaction heating rate in the experimental methods.[14,15,48,52,53] This is surprising for the chelate decomposition method, in particular, given the general acceptance that the reaction is governed by the controlled release of calcium into solution.[15,19–22] Therefore, we hypothesized that the whisker morphology should be governed, in large part, by the kinetics of chelate decomposition. Moreover, the objective of this study was to investigate purely kinetic effects, such as the reaction heating and stirring rate, on the morphology of HA whiskers synthesized using the chelate decomposition method in order to offer new insights and provide clarification regarding the reaction mechanism.

II. Experimental Procedure

(1) HA Whisker Synthesis

HA whiskers were synthesized from aqueous solutions containing DL-lactic acid ($C_3H_6O_3$, Sigma Chemical Co., St. Louis, MO), phosphoric acid (H_3PO_4, Sigma Chemical Co.), and calcium hydroxide ($Ca(OH)_2$, Aldrich Chemical Company Inc., Milwaukee, WI). All chemicals were ACS reagent grade. 0.10*M* lactic acid and 0.03*M* phosphoric acid were added to deionized water, followed by dissolving 0.05*M* calcium hydroxide under constant stirring for 2 h. A homogeneous solution with pH = 4.0 was filtered and stored in a bottle purged with nitrogen. Note that the molar ratio of Ca to P in the solution was 1.67, which is equivalent to that of stoichiometric HA.

HA whiskers were precipitated from the solution under hydrothermal conditions. 1250 mL of the solution was placed in the Teflon® liner of a 2 L pressure vessel (Model 4600, Parr Instrument Co., Moline, IL) and purged with nitrogen. In order to provide uniform thermal transport, 250 mL of de-ionized water was placed in the gap between the liner and stainless-steel vessel. Reaction conditions were controlled by a heating assembly (Model 4910, Parr Instrument Co.) and temperature controller (Model 4840, Parr Instrument Co.). The reaction temperature was measured by a thermocouple placed inside a thermowell in the vessel. Upon completion of each reaction, the vessel was cooled to ambient conditions within 1 h using a cooling fan. HA precipitates were collected from the solution by vacuum filtration, and the pH of the supernatant solution was measured. The HA precipitates were then washed under constant flow with 1250 mL de-ionized water and dried in an oven at 90°C for at least 12 h.

In order to study the kinetic effects on the morphology of HA whiskers, three experimental parameters were investigated independently: the reaction heating rate, stirring rate, and temperature. For heating and stirring rate experiments, all reactions were heated to 200°C and held for 2 h. The autogenous pressure reached a maximum of 14 MPa at 200°C. Reaction solutions were heated to the final temperature in 1, 2, 4, and 8 h, corresponding to heating rates of 3.0°, 1.4°, 0.75°, and 0.36°C/min, respectively, as measured by linear regression over the temperature range 110°–190°C ($R^2 > 0.99$). For the 1.4°C/min heating rate, solutions were stirred at 0 (static), 50, 150, and 250 rpm during the reaction. In order to investigate more closely the reaction mechanism during heating, reaction solutions were heated at 1.4° and 0.75°C/min under static conditions to a final temperature of 80°, 100°, 120°, 140°, 160°, 180°, and 200°C, and held for 2 h.

(2) Morphology

The size and morphology of HA whiskers was characterized quantitatively using an optical microscope (Eclipse ME600L, Nikon Instruments, Inc., Melville, NJ) equipped with a digital camera (Magnafire, Olympus America, Melville, NJ) connected to a personal computer with imaging software (Object-Image 2.08). Samples were prepared by ultrasonically dispersing 0.003 g of HA precipitates in 1 mL of methanol. Drops of the suspension were pipetted onto a pre-heated glass slide in an oven at 90°C to evaporate the alcohol quickly. All samples were examined at $\times 400$ magnification using transmitted light. A 10×10 square grid was digitally overlaid using the imaging software in order to facilitate random selection of precipitates. The length and the width were measured for each precipitate located at grid intersections, and the aspect ratio (length/width) was calculated. Five hundred precipitates were measured for each sample.

One-way analysis of variance (ANOVA) (Statview 5.01, SAS Institute Inc., Cary, NC) was used to compare the mean length, width, and aspect ratio of HA whiskers synthesized for each experimental group. *Post hoc* comparisons were performed using Student's *t*-test. A log transform of the data was used to provide a normal distribution for statistical analyses.

HA precipitates prepared at 150 and 250 rpm stirring contained crystals that were too small for accurate characterization using optical microscopy. Therefore, the size and morphology of these powders were qualitatively characterized using field-emission scanning electron microscopy (FESEM) with an accelerating voltage of 20 kV and a working distance of 9 mm (S-4500, Hitachi High-Technologies Corporation, Tokyo, Japan). Precipitates were deposited onto the SEM sample holder using the same technique described above for optical microscopy and coated with gold by sputter deposition.

(3) Crystallographic Phase and Composition

The crystallographic phase and composition of all precipitates was determined by powder X-ray diffraction (XRD), using Cu$K\alpha$ radiation generated at 40 kV and 30 mA (X-1, Scintag Inc., Cupertino, CA). In order to minimize the effects of preferred orientation, all powders were ground using a mortar and pestle, and placed in a side loading sample holder. For phase identification, powders were examined over 10°–60° 2θ with a step size of 0.02° and step time of 0.5 s.

Quantitative analysis was used to determine the relative amounts of HA and DCPA, $CaHPO_4$, if present, in the reaction products. Known mixtures of as-synthesized HA whiskers and a DCPA powder (S79947, Fisher Scientific, Chicago, IL) exhibited a linear relationship between the weight fraction of HA in the mixture and the integrated intensity ratio of the (211) HA reflection and the (120) DCPA reflection ($R^2 = 0.995$). Thus, the amount of HA in reaction products was determined as

$$f_{HA} = \frac{I_{HA}}{I_{HA} + I_{DCPA}} \quad (1)$$

where f_{HA} is the weight fraction of HA in the mixture, I_{HA} is the integrated intensity of the (211) HA reflection, and I_{DCPA} is the integrated intensity of the (120) DCPA reflection. Diffraction patterns of these reflections were collected over 29.5° –32.1° 2θ with a step size of 0.02° and a step time of 5.0 s. The total reaction yield (wt% Ca) was determined gravimetrically from the mass of precipitates collected by vacuum filtration, combined with the measured weight fractions of HA and DCPA. The residual calcium concentration in the supernatant solution was also measured using a calcium ion-selective electrode (ISE) and reference electrode (Models 50240 and 50240, Hach Co., Loveland, CO).

The Ca/P ratio in HA precipitates was determined from the amount of β-tricalcium phosphate (β-TCP), β-$Ca_3(PO_4)_2$, formed after heat treatment.[65–68] Approximately 0.5 g of single-phase reaction products (no DCPA present) was heated to 1000°C for 10 h and examined by quantitative analysis using XRD. Known mixtures of as-synthesized HA whiskers and a β-TCP powder (21218, Fluka Chemika, Germany) exhibited a linear relationship between the weight fraction of β-TCP in the mixture and the integrated intensity ratio of the (210) β-TCP reflection and (211) HA reflection ($R^2 = 0.987$). Thus, the amount of β-TCP in reaction products was determined as

$$f_{\beta-TCP} = \frac{I_{\beta-TCP}}{I_{\beta-TCP} + I_{HA}} \quad (2)$$

where $f_{\beta\text{-TCP}}$ is the weight fraction of β-TCP in the mixture, $I_{\beta\text{-TCP}}$ is the integrated intensity of the (210) β-TCP reflection, and I_{HA} is the integrated intensity of the (211) HA reflection. Diffraction patterns of these reflections were collected over 30.5°–32.1° 2θ with a step size of 0.02° and a step time of 10 s. Finally, the Ca/P ratio was calculated as

$$\frac{Ca}{P} = \frac{\frac{10\cdot(1-f_{\beta-TCP})}{M_{HA}} + \frac{3\cdot f_{\beta-TCP}}{M_{\beta-TCP}}}{\frac{6\cdot(1-f_{\beta-TCP})}{M_{HA}} + \frac{2\cdot f_{\beta-TCP}}{M_{\beta-TCP}}} \quad (3)$$

where $f_{\beta\text{-TCP}}$ is the weight fraction of β-TCP in the heat-treated powder, M_{HA} is the molar weight for stoichiometric HA, and $M_{\beta\text{-TCP}}$ is the molar weight for stoichiometric β-TCP.[68] Note that a rigorous previous investigation determined the absolute uncertainty of Ca/P ratios measured using a nearly identical technique to range from ±0.001 to ±0.006 for Ca/P < 1.667.[68] A 95% confidence interval was calculated for the Ca/P ratio as a function of the β-TCP weight fraction in order to test for statistically significant differences between measurements.

The composition of reaction products was also examined using a Fourier transform–infrared (FT-IR) spectrometer (Nicolet IR200, Thermo Electron Corporation, Waltham, MA). In order to achieve adequate transmittance, HA precipitates were mixed with potassium bromide (KBr, FT-IR grade, Aldrich Chemical Company, Inc., Milwaukee, WI) in a 1:15 ratio by mass using a mortar and pestle. A thin pellet of the mixture was formed in an evacuated die under 200 MPa uniaxial pressure. Spectra were obtained over frequencies of 4000–500 cm^{-1} and normalized to the background spectra for a KBr pellet alone.[69,70]

III. Results

(1) Heating Rate Effects

The effects of the reaction heating rate were investigated under static conditions, heating at 3.0°, 1.4°, 0.75°, and 0.36°C/min to a final temperature of 200°C, which was held for 2 h. The solution pH became more acidic after the reaction and the change in solution pH decreased from −0.97 to −0.92 with decreased heating rate (Table I). No phases other than HA were detected by XRD and no differences were observed between heating rates (Fig. 1). FT-IR spectra confirmed the presence of hydroxyl (OH) groups, as well as HPO_4 substituents (Fig. 2). A decreased heating rate resulted in slightly increased OH peaks and decreased HPO_4 peaks. Ca/P ratios increased from 1.58 to 1.62 with decreased heating rate over the range in this study (Table I).

Table I. Effects of the Reaction Heating Rate on the Solution pH and Ca/P Ratio

Heating Rate (°C/min)	Temperature (°C)	ΔpH	$\frac{Ca}{P}$
0.36	200	−0.92	1.62†
0.75	200	−0.91	1.60
1.4	200	−0.94	1.59
3.0	200	−0.97	1.58†

†Statistically significant difference from all other groups (95% confidence interval).

The morphology of HA precipitated at each heating rate was whisker like, as shown by the optical micrographs in Fig. 3. The number of fine powder particles decreased and the mean length of whiskers increased with decreased heating rate (Fig. 3). The mean length and aspect ratio of the whiskers increased approximately twofold with decreased heating rate over the range studied (Fig. 4). Statistically significant differences were measured between each heating rate ($p < 0.0001$). The mean whisker width decreased with decreased heating rate, but was much less influenced (Fig. 4(a)). Statistically significant differences were measured between 0.36°C/min and all other heating rates ($p < 0.0001$), as well as between 0.75° and 3.0°C/min ($p < 0.05$). Thus, variation in the whisker aspect ratio was primarily due to variation in the whisker length.

(2) Stirring Rate Effects

The effects of the reaction stirring rate were investigated at 0, 50, 150, and 250 rpm stirring, heating at 1.4°C/min to a final temperature of 200°C, which was held for 2 h. The change in solution pH was −0.92, −1.05, −1.31, and −1.25 for 0, 50, 150, and 250 rpm stirring, respectively. No phases other than HA were detected by XRD for each stirring rate (Fig. 1). FT-IR spectra confirmed the presence of hydroxyl (OH) groups, as well as HPO_4 substituents (Fig. 2). A decreased stirring rate resulted in slightly increased OH peaks and decreased HPO_4 peaks. The Ca/P ratio was 1.59 and was not statistically different (95% confidence interval) between static conditions (0 rpm) and the maximum stirring rate (250 rpm).

The morphology of HA precipitated at each stirring rate ranged from micro-scale whiskers under static conditions to

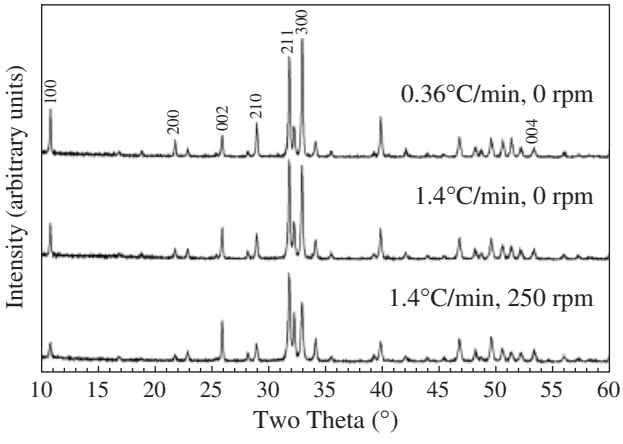

Fig. 1. X-ray diffraction patterns for hydroxyapatite (HA) precipitated at a final temperature of 200°C, which was held for 2 h, showing the effects of selected heating and stirring rates. All reflections correspond to HA.

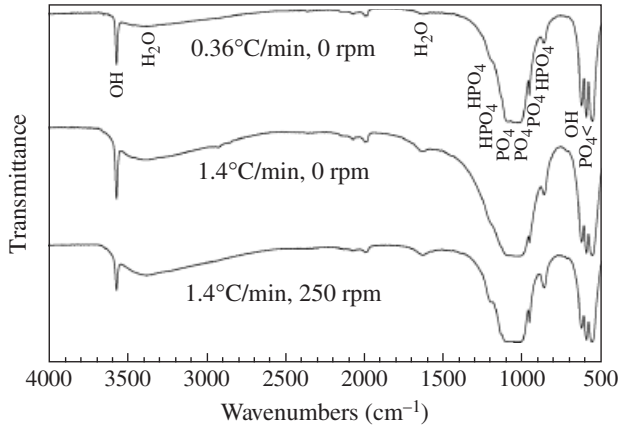

Fig. 2. Fourier transform infrared spectra for hydroxyapatite precipitated at a final temperature of 200°C, which was held for 2 h, showing the effects of selected heating and stirring rates.

nano-scale plates under rapid stirring, as shown by the scanning electron micrographs in Fig. 5. The mean length and width of the whiskers decreased with increased stirring rate for static conditions and 50 rpm stirring, while the aspect ratio was not statistically different (Table II). The smaller size and altered morphology of HA precipitates prepared at 150 and 250 rpm stirring prohibited quantitative characterization and comparison using the above methods.

(3) Temperature Effects

The effects of the reaction temperature were investigated under static conditions, heating at 1.4° or 0.75°C/min to a final temperature of 80°, 100°, 120°, 140°, 160°, 180°, and 200°C, which was held for 2 h. The trends described below were similar for each heating rate. The change in solution pH increased with

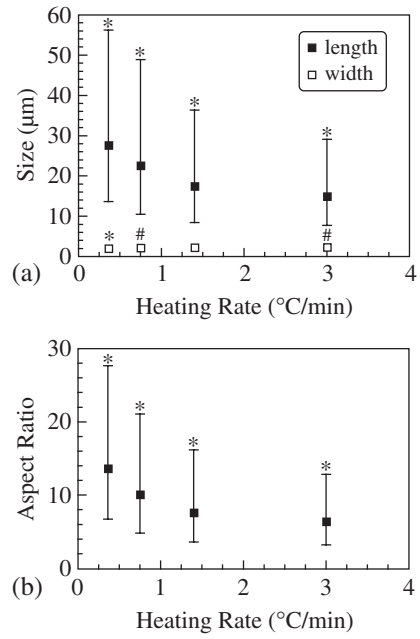

Fig. 4. Effects of the reaction heating rate on the hydroxyapatite whisker (a) length, width, and (b) aspect ratio, showing the mean and first standard deviation using a log-normal transform of the data. Statistically significant differences, $p<0.0001$ (*) and $p<0.05$ (#), existed between heating rates. All reactions were heated under static conditions to a final temperature of 200°C, which was held for 2 h.

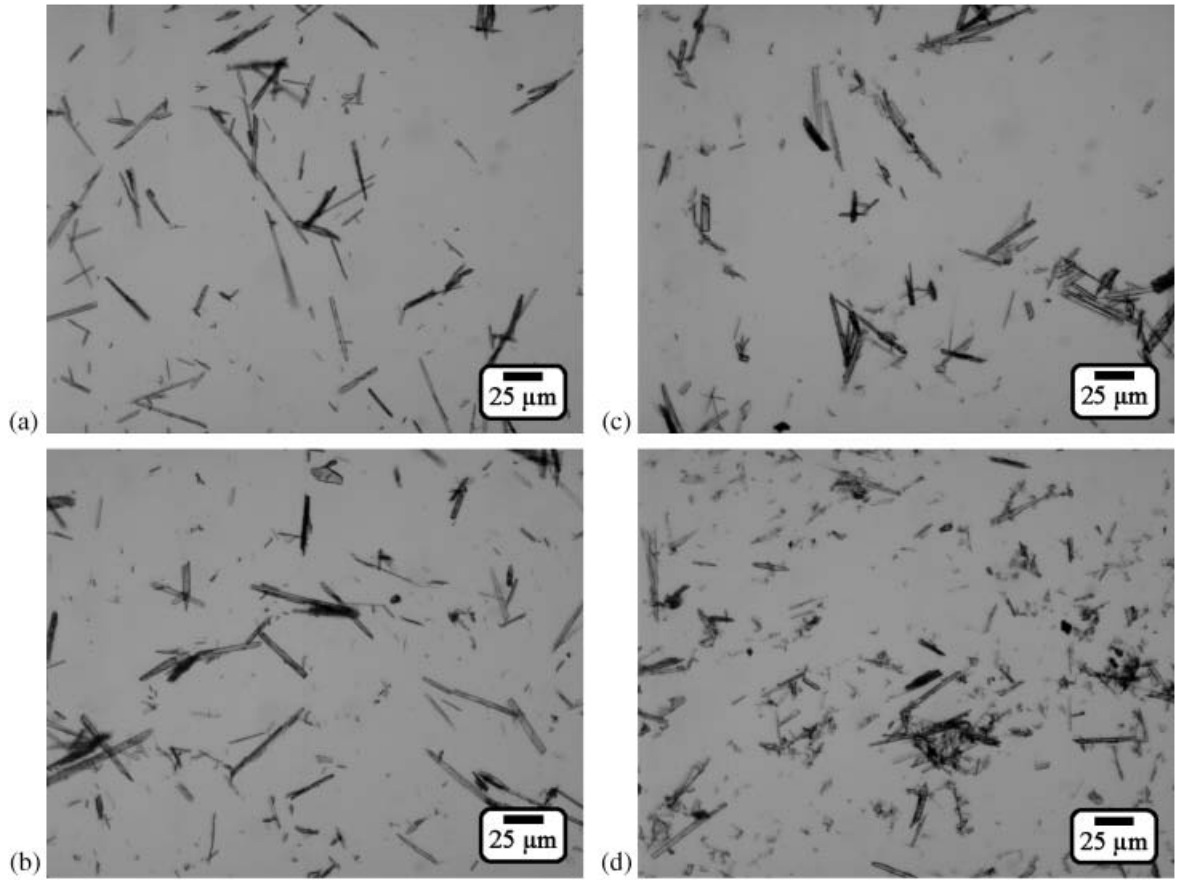

Fig. 3. Transmitted light micrographs for hydroxyapatite (HA) precipitated under static conditions, heating at (a) 0.36°C/min, (b) 0.75°C/min, (c) 1.4°C/min, and (d) 3.0°C/min to a final temperature of 200°C, which was held for 2 h, showing the effects of the reaction heating rate on the HA whisker morphology.

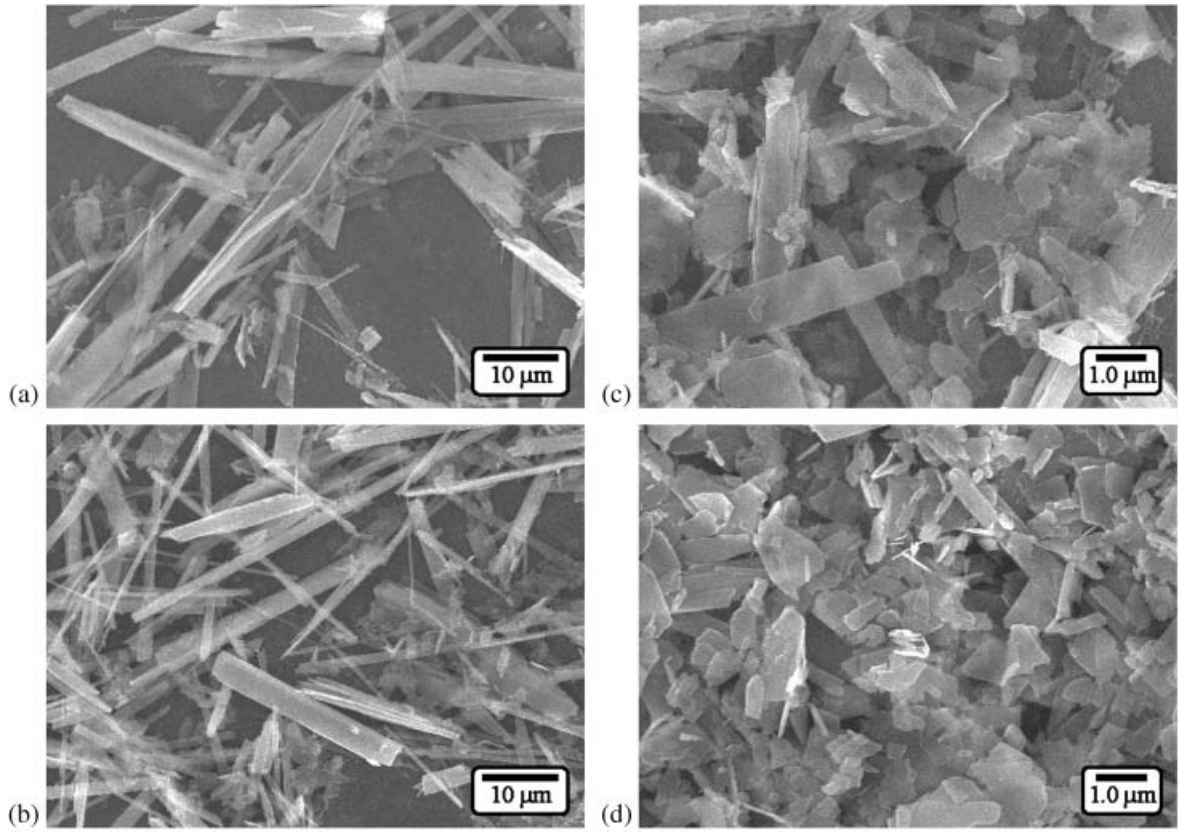

Fig. 5. Scanning electron micrographs for hydroxyapatite (HA) precipitated under (a) 0 rpm, (b) 50 rpm, (c) 150 rpm, and (d) 250 rpm stirring, heating at 1.4°C/min to a final temperature of 200°C, which was held for 2 h, showing the effects of the reaction stirring rate on the HA crystal morphology.

increased reaction temperature. At 1.4°C/min, the change in solution pH was −0.09, −0.33, −0.49, −0.67, −0.80, −0.95, and −1.03 for 80°, 100°, 120°, 140°, 160°, 180°, and 200°C, respectively. No measurable reaction products were detected at 80°C. At the initial stages of the reaction (100°–120°C), small amounts of precipitates were formed that were predominantly DCPA, as well as HA (Figs. 6 and 7). XRD reflections for HA were observed at 100°C (Fig. 6), but FT-IR did not detect a hydroxyl (OH) band until 120°C (Fig. 8). By 160°C, precipitates consisted almost entirely of HA, with less than 0.3 wt% DCPA remaining (Fig. 7). At 180°–200°C, no phases other than HA were detected by XRD (Fig. 6). The total reaction yield reached a maximum of approximately 70 wt% Ca at 200°C (Fig. 7), indicating that calcium remained in the supernatant solution following the reaction. There was good agreement between the total reaction yield measured both gravimetrically and by the residual calcium concentration in the supernatant solution using a calcium ISE. FT-IR spectra confirmed the presence of HPO_4 substituents in all precipitates (Fig. 9). Increased reaction temperature resulted in slightly increased OH peaks and decreased HPO_4 peaks. Ca/P ratios significantly increased (95% confidence interval) from 1.57–1.58 at 160°C to 1.60–1.61 at 180°C. Further increases in the Ca/P ratio from 180° to 200°C were not statistically significant. Finally, increased heating rate resulted in an increased precipitation rate, with the maximum precipitation rate occurring between 120° and 140°C for either heating rate.

The morphology of HA precipitated at each reaction temperature under static conditions was whisker like, with no

Table II. Effects of the Reaction Stirring Rate on Hydroxyapatite Whisker Morphology

Stirring Rate (rpm)	Length† (μm)	Width† (μm)	Aspect Ratio†
0	17.5 (+18.8/−9.0)	2.3 (+1.0/−0.7)	7.6 (+8.6/−4.0)
50	15.5 (+16.2/−7.9)	2.0 (+0.7/−0.5)	7.6 (+8.5/−4.0)
p	<0.01	<0.0001	0.94

†Mean ± standard deviation determined using a log-normal transform of the data.

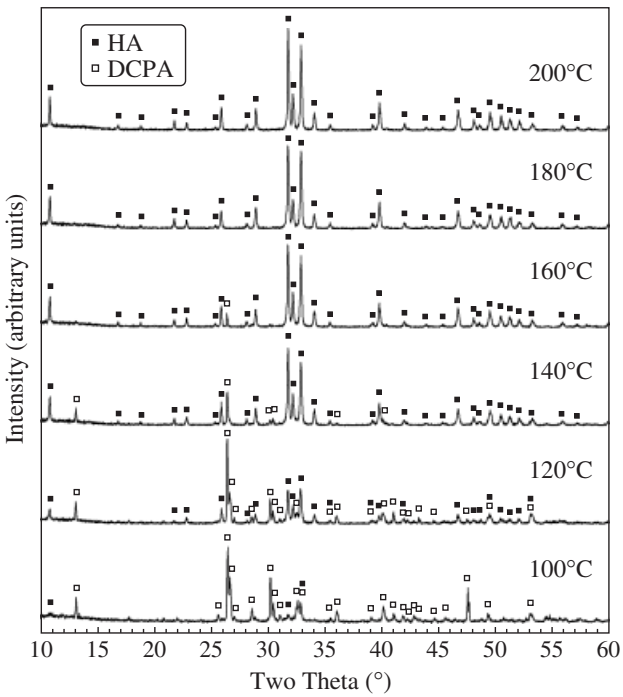

Fig. 6. X-ray diffraction patterns for hydroxyapatite precipitated under static conditions, heating at 1.4°C/min, showing the effects of the reaction temperature.

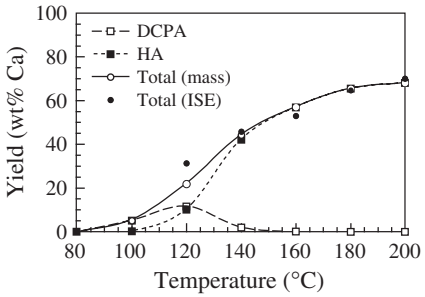

Fig. 7. Total reaction yield (wt% Ca) for hydroxyapatite (HA) precipitated under static conditions, heating at 1.4°C/min, showing the effects of the reaction temperature. The reaction yield was measured both gravimetrically and using a calcium ion-selective electrode (ISE). Phase fractions for DCPA and HA were determined by quantitative X-ray diffraction analysis.

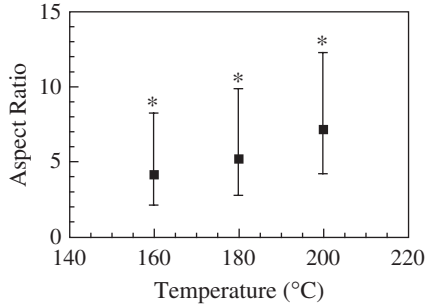

Fig. 9. Effects of the reaction temperature on the hydroxyapatite whisker aspect ratio, showing the mean and first standard deviation using a log-normal transform of the data. Statistically significant differences, $p<0.0001$ (*), existed between each reaction temperature. All reactions were heated at 1.4°C/min under static conditions and held at the final temperature, which was held for 2 h.

qualitative differences from that at 200°C using the same heating rate (Figs. 3(b), (c), and 5(a)). Quantitative comparisons were possible for phase-pure HA precipitates synthesized at 160°–200°C. Over this range, the mean length and aspect ratio of the whiskers increased with increased reaction temperature (Fig. 9). Statistically significant differences were measured between each reaction temperature ($p<0.0001$).

IV. Discussion

(1) Kinetic Effects on Morphology

The length and aspect ratio of HA whiskers precipitated using the chelate decomposition method increased with decreased heating rate (Figs. 3 and 4), decreased stirring rate (Fig. 5 and Table II), and increased reaction temperature (Fig. 9). The most significant effects were due to changes in the heating and stirring rates. The mean length and aspect ratio of whiskers increased approximately twofold with decreased heating rate over the range studied (Fig. 4). Therefore, the reaction heating rate is a key variable that can be used to tailor the morphology of HA whiskers and ought to be reported in future investigations. As added evidence to the importance of the reaction heating rate, Katsuki *et al.*[56] showed that the morphology of HA, precipitated by hydrolysis of a calcium sulfate precursor, was altered from whisker-like using conventional heating to plate-like using microwave heating. Although heating rates were not reported, microwave heating certainly provided a much faster heating rate than was possible by the conventional heating used in either their study or this investigation. Furthermore, at the other extreme and as noted in the introduction, single-crystal HA whiskers up to 1 cm long have been grown using sintered HA seeds to control nucleation, and multiple heating zones to control heat transfer and convective flow in a pressure vessel.[52,53] The heating rates reported in these investigations ranged from 0.10° to 0.005°C/min, much lower than those implemented in this investigation. Considering these studies together with the data in this investigation, the length or aspect ratio of HA whiskers is inversely related to the reaction heating rate by a power law as

$$\text{whisker length or aspect ratio} = K \cdot \left(\frac{dT}{dt}\right)^{-n} \tag{4}$$

where dT/dt is the heating rate and K and n are constants. For data in Fig. 4, $K = 20.3$ and $n = 0.30$ for whisker length ($R^2 = 0.98$); $K = 9.2$ and $n = 0.36$ for the whisker aspect ratio ($R^2 = 0.99$). Thus, the results of this study suggest a general relationship:

$$\text{whisker length or aspect ratio} \approx K \cdot \left(\frac{dT}{dt}\right)^{-1/3} \tag{5}$$

The reaction heating rate and temperature had relatively little effect on the width of HA whiskers; however, the precipitate morphology was significantly altered from micro-scale whiskers to nano-scale plates with increased stirring rate (Fig. 5). High-resolution transmission electron microscopy and electron diffraction investigations have previously confirmed that HA whiskers are single-crystal hexagonal prisms elongated in the *c*-axis <001> with exposed *a*-planes {210}.[15,16,20,37,38,57] Plate-like HA crystals, whether synthetic or biological (e.g., apatite bone mineral), are elongated by length in the *c*-axis and by width in the *a*-axis, with the plate faces approximately corresponding to {100} planes.[71–73] Thus, the crystal morphology was dramatically altered by reaction kinetics, independent of changes in the solution chemistry. Furthermore, the similarity of synthetic plate-like HA crystals to apatite crystals in bone[72] suggests that the morphology of biological apatites may be governed by kinetics and that mineralization *in vivo* may occur rather rapidly.

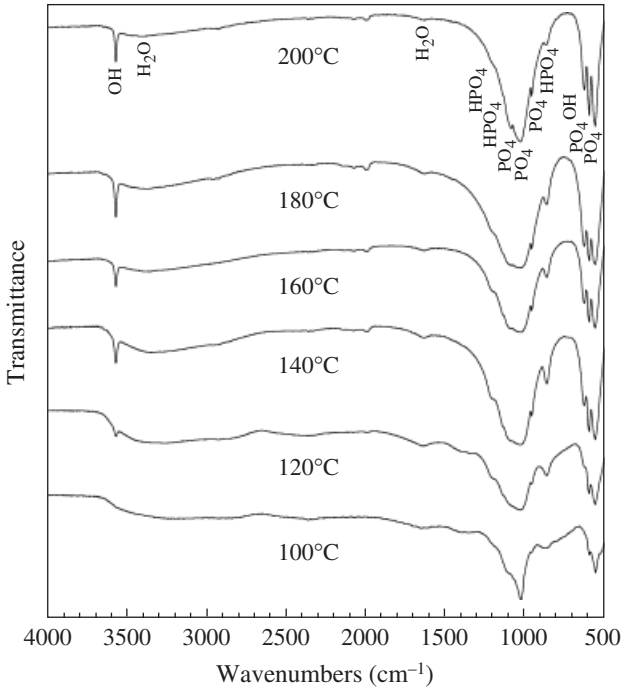

Fig. 8. Fourier transform infrared spectra for hydroxyapatite precipitated under static conditions, heating at 1.4°C/min, showing the effects of the reaction temperature.

(2) Kinetic Effects on Crystal Chemistry

FT-IR spectra showed that a decreased heating or stirring rate resulted in increased OH peaks and decreased HPO_4 peaks (Fig. 2). The Ca/P ratio measured by quantitative XRD increased with decreased heating rate (Table I), but was not affected by the stirring rate. Therefore, decreased reaction kinetics resulted in increased order in the HA crystal structure. Similar effects were observed due to changes in the thermodynamic driving force. An increased reaction temperature resulted in increased OH peaks, decreased HPO_4 peaks (Fig. 8), and increased Ca/P ratio. Thus, increased structural order was achieved by either decreasing the reaction kinetics or increasing the thermodynamic driving force. Under the conditions examined in this study, kinetic effects were just as strong, if not stronger, than thermodynamic effects. These results suggest that the formation of disordered, calcium-deficient apatites in both synthetic and biological systems is dependent on kinetic effects in addition to classical thermodynamic arguments.[74]

(3) Reaction Mechanism

There is general agreement that the growth of HA whiskers by the chelate decomposition method is facilitated by the controlled release of calcium ions into solution.[15,19–21] In this study, the maximum precipitation rate for HA occurred over 120°–140°C (Fig. 7), which was indicative of the kinetics for the chelate decomposition. Thus, the reaction kinetics were governed by the following chemical equilibria:

$$[CH_3CH(OH)COO]Ca^+ + H^+ \leftrightharpoons CH_3CH(OH)COOH + Ca^{2+} \quad (6)$$

Calcium ions were released into solution as the above equilibria was shifted to the right by concomitant changes in pH, temperature, and/or concentration. The stability constant (pK_a) for lactic acid is 3.86 at 25°C.[75] Therefore, a decrease in pH would be expected to coincide with the release of calcium ions into solution. In this study, reaction solutions were prepared at pH = 4 and were measured to decrease to pH ≈ 3 after precipitation. Furthermore, the boiling point of lactic acid has been reported to be in the range of 100°–140°C (7–27 kPa).[76,77] Thus, these observations suggest that increased temperature led to decomposition and decreased concentration of the calcium carboxylate chelate, decreased pH, and increased free calcium concentration. However, further work is needed to calculate species distribution diagrams[78] or stability diagrams[79] at elevated temperature. In other methods for HA whisker synthesis, the rate-limiting chemical equilibria may be that of the decomposition of urea, which raises solution pH, or the hydrolysis of a particular calcium phosphate precursor.

The results of this study offer new insights and provide clarification regarding the reaction mechanism for HA whisker synthesis using the chelate decomposition method. Before the nucleation of HA, the reaction solution was undersaturated with respect to all calcium phosphate phases through the use of a chelating agent (e.g., carboxylic acid) to bind calcium ions in solution. Note that without the chelating agent, the solution would have been supersaturated and the most stable calcium phosphate phase would have spontaneously precipitated. As the pressure vessel containing this homogeneous solution was heated from an external source, a temperature gradient was formed across the reactor wall (Fig. 10(a)). Therefore, calcium carboxylates began to decompose near the reactor wall, according to the equilibria of Eq. (6). As the solution became locally supersaturated, heterogeneous nucleation of HA (or a DCPA precursor) occurred at the reactor wall (Fig. 10(a)). Note that under certain conditions, we have visually observed a felt-like appearance on the Teflon liner due to the presence of HA whiskers, which had to be removed by scraping the reactor wall. We have also observed that altering the surface roughness of the reactor wall influences the whisker morphology, presumably by altering the nucleation rate or nuclei size. These observations support a heterogeneous nucleation mechanism and also suggest that the frequent use of "homogenous precipitation" in the literature may be misleading.[17,19,23] Finally, the controlled growth of HA nuclei at the reactor wall was facilitated by the controlled heat flux across the reactor wall into the solution and the concomitant diffusion of released calcium ions toward the HA nuclei or crystallites (Fig. 10(b)).

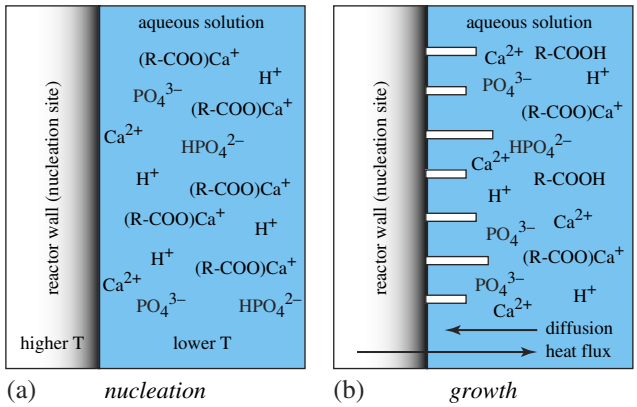

Fig. 10. Schematic illustration of the reaction mechanism for hydroxyapatite whisker (a) nucleation and (b) growth using the chelate decomposition method. Note that R = $CH_3CH(OH)$ for lactic acid.

In light of the above description of the reaction mechanism, the kinetic effects of the heating rate, stirring rate, and reaction temperature on the whisker morphology are apparent. Under static conditions at a fixed final reaction temperature, a decreased heating rate resulted in a slower release of calcium ions from the solution and a decreased nucleation rate of crystals (fewer number of nuclei), which, due to a fixed reactant concentration in solution and equilibrium constant for Eq. (6), were able to grow to a greater length and aspect ratio (Figs. 3 and 4). For a fixed heating rate and final reaction temperature, an increased stirring rate resulted in a cascade of effects: (1) controlled heat and diffusion gradients in the solution were disrupted—in other words, the solution temperature and calcium concentration were homogenized throughout—leading to a rapid release of calcium ions from solution and an increased nucleation rate, (2) crystals nucleating at the reactor wall were swept away before significant growth, and (3) the above effects led to heterogeneous nucleation throughout the reaction solution, or perhaps even homogeneous nucleation. Thus, an increased stirring rate resulted in a dramatic decrease in the size and a change in the morphology of the HA precipitates from micro-scale whiskers to nano-size plates (Fig. 5). For a fixed heating rate under static conditions, an increased final reaction temperature above 160°C resulted in increased crystal growth. Increased growth was evident in that the percent increase in the mean whisker length or aspect ratio (noting that changes in the width were relatively insignificant) was several times greater than the percent increase in the reaction yield over 160°–200°C (Figs. 7 and 9).

While the results of this study clearly elucidate kinetic effects on the HA whisker morphology and reaction mechanism, other effects remain less clear. Small amounts of DCPA crystals nucleated before HA (Figs. 6 and 7). Whether DCPA was transient, or a precursor to HA through dissolution-reprecipitation or phase transformation, cannot be determined from the results of this study alone. Interestingly, the existence and identification of precursor phases, such as DCPA, ACP and octacalcium phosphate (OCP), to biological apatite have been controversial.[80] The effects of selective molecular binding to crystal faces are also uncertain in this study. The selective binding of molecules—including carboxylic acids, carbohydrates, and proteins—to specific crystal faces has been proposed as a means to tailor crystal growth and particle morphology.[25,27,38,81–84]

Direct evidence for binding of various molecules to HA has been documented,[73,83,84] but attributing morphological control to these observations is not straightforward. For example, Walsh *et al.* showed that morphological changes in precipitated HA whiskers were correlated to the stability of the interaction of monosaccharides with calcium; however, the observation of similar morphological effects in the absence of the additives suggested that the effects were kinetic rather than due to selective surface binding.[38] In other words, molecules that can bind to crystals also have concomitant effects on the chemical solution equilibria (Eq. (6)) and the kinetics of chelate decomposition. Finally, the aggregative growth mechanism proposed by Kandori *et al.*[23] cannot be unequivocally ruled out by this study, but the observation that relatively large HA whiskers were formed even at low reaction yields (e.g., 120°C) suggests that aggregative growth was unlikely.

V. Conclusions

HA whiskers synthesized by the chelate decomposition method were a phase-pure, calcium-deficient apatite (Ca/P = 1.57–1.62) with HPO_4 substituents. Disorder in the HA crystal structure was promoted by an increased heating rate, increased stirring rate, and decreased temperature. Small amounts of DCPA formed during the initial stages of the reaction (100°–120°C), but were no longer detected by the time the reaction was complete (180°–200°C). The maximum precipitation rate of HA occurred over 120°–140°C, as governed by the kinetics of chelate decomposition.

The length and aspect ratio of HA whiskers increased with decreased heating rate, decreased stirring rate, and increased reaction temperature. The mean length and aspect ratio of HA whiskers increased approximately twofold with decreased heating rate over the range studied, following a power-law relationship. Decreased heating rate resulted in a slower release of calcium ions from the solution and a decreased nucleation rate of crystals (fewer number of nuclei), which were able to grow to a greater length and aspect ratio. Therefore, the reaction heating rate is a key variable that can be used to tailor the morphology of HA whiskers and ought to be reported in the literature. The reaction heating rate and temperature had relatively little effect on the width of HA whiskers. However, the precipitate morphology was altered significantly from micro-scale whiskers to nano-scale plates with increased stirring rate. Increased stirring rate disrupted heat and diffusion gradients in the solution, leading to the rapid release of calcium ions from solution, an increased nucleation rate, and decreased crystal growth. Finally, increased reaction temperature above 160°C resulted in increased crystal growth.

References

[1]R. Z. LeGeros and J. P. LeGeros, "Dense Hydroxyapatite"; pp. 139–80 in *Advanced Series in Ceramics*, Vol. 1, An Introduction to Bioceramics. Edited by L. L. Hench and J. Wilson. World Scientific Publishing Co., New Jersey, 1993.

[2]L. L. Hench, "Bioceramics: From Concept to Clinic," *J. Am. Ceram. Soc.*, **74** [7] 1487–510 (1991).

[3]R. Holmes, V. Mooney, R. Bucholz, and A. Tencer, "A Coralline Hydroxyapatite Bone Graft Substitute," *Clin. Orthop. Rel. Res.*, [188] 252–6 (1984).

[4]H. Oguchi, K. Ishikawa, K. Mizoue, K. Seto, and G. Eguchi, "Long-Term Histological Evaluation of Hydroxyapatite Ceramics in Humans," *Biomaterials*, **16**, 33–8 (1995).

[5]W. Suchanek, M. Yashima, M. Kakihana, and M. Yoshimura, "Processing and Mechanical Properties of Hydroxyapatite Reinforced with Hydroxyapatite Whiskers," *Biomaterials*, **17** [17] 1715–23 (1996).

[6]W. Suchanek, M. Yashima, M. Kakihana, and M. Yoshimura, "Hydroxyapatite/Hydroxyapatite–Whisker Composites Without Sintering Additives: Mechanical Properties and Microstructural Evolution," *J. Am. Ceram. Soc.*, **80** [11] 2805–13 (1997).

[7]W. L. Suchanek and M. Yoshimura, "Preparation of Fibrous, Porous Hydroxyapatite Ceramics from Hydroxyapatite Whiskers," *J. Am. Ceram. Soc.*, **81** [3] 765–7 (1998).

[8]R. K. Roeder, M. M. Sproul, and C. H. Turner, "Hydroxyapatite Whisker Reinforcements Used to Produce Anisotropic Biomaterials," *Trans. Orthop. Res. Soc.*, **26**, 528 (2001).

[9]R. K. Roeder, M. S. Sproul, and C. H. Turner, "Hydroxyapatite Whiskers Provide Improved Mechanical Properties in Reinforced Polymer Composites," *J. Biomed. Mater. Res.*, **67A** [3] 801–12 (2003).

[10]J.-Y. Rho, L. Kuhn-Spearing, and P. Zioupos, "Mechanical Properties and the Hierarchical Structure of Bone," *Med. Eng. Phys.*, **20**, 92–102 (1998).

[11]H.-R. Wenk and F. Heidelbach, "Crystal Alignment of Carbonated Apatite in Bone and Calcified Tendon: Results from Quantitative Texture Analysis," *Bone*, **24** [4] 361–9 (1999).

[12]R. Z. LeGeros, O. R. Trautz, J. P. LeGeros, E. Klein, and W. P. Shirra, "Apatite Crystallites: Effects of Carbonate on Morphology," *Science*, **155**, 1409–11 (1967).

[13]D. R. Simpson, "Substitutions in Apatite: I. Potassium-Bearing Apatite," *Am. Mineral.*, **53** [3–4] 432–44 (1968).

[14]T. Hattori, Y. Iwadate, and T. Kato, "Hydrothermal Synthesis of Hydroxyapatite form Calcium Acetate and Triethyl Phosphate," *Adv. Ceram. Mater.*, **3** [4] 426–8 (1988).

[15]N. Christiansen and R. E. Riman, "Bioceramics—A Future Through Microstructural and Chemical Design"; pp. 209–20 in *Proceedings of the 5th Scandinavian Symposium on Materials Science, New Materials and Processes May 22–25, 1989*, Edited by I. L. H. Hansson and H. Lilhot. Danish Society for Materials Testing and Research, Copenhagen, Denmark, 1989.

[16]M. Yoshimura, H. Suda, K. Okamoto, and K. Ioku, "Hydrothermal Synthesis of Needle-like Apatite Crystal," *Nippon Kagaku Kaishi*, **10**, 1402–7 (1991).

[17]M. Toriyama, Y. Kawamoto, T. Suzuki, Y. Yokogawa, K. Nishizawa, and H. Nagae, "Synthesis of Hydroxyapatite by an Oxidative Decomposition Method of Calcium Chelate," *J. Ceram. Soc. Jap.*, **100** [7] 950–4 (1992).

[18]M. Yoshimura, K. Ioku, K. Okamoto, and H. Takeuchi, "Apatite Whisker and Method for Preparation Thereof"; U.S. Pat. No. 5 227 147, 1993.

[19]Y. Fujishiro, H. Yabuki, K. Kawamura, T. Sato, and A. Okuwaki, "Preparation of Needle-Like Hydroxyapatite by Homogeneous Precipitation Under Hydrothermal Conditions," *J. Chem. Technol. Biotechnol.*, **57**, 349–53 (1993).

[20]M. Yoshimura, H. Suda, K. Okamoto, and K. Ioku, "Hydrothermal Synthesis of Biocompatible Whiskers," *J. Mater. Sci.*, **29**, 3399–402 (1994).

[21]W. Suchanek, H. Sada, M. Yashimi, M. Kakihana, and M. Yoshimura, "Biocompatible Whiskers with Controlled Morphology and Stoichiometry," *J. Mater. Res.*, **10** [3] 521–9 (1995).

[22]N. Asaoka, H. Suda, and M. Yoshimura, "Preparation of Hydroxyapatite Whiskers by Hydrothermal Method," *J. Chem. Soc. Jpn.*, **1**, 25–9 (1995).

[23]K. Kandori, N. Horigami, A. Yasukawa, and T. Ishikawa, "Texture and Formation Mechanism of Fibrous Calcium Hydroxyapatite Particles Prepared by Decomposition of Calcium-EDTA Chelates," *J. Am. Ceram. Soc.*, **80** [5] 1157–64 (1997).

[24]S. Suzuki, M. Ohgaki, M. Ichiyanagi, and M. Ozawa, "Preparation of Needle-Like Hydroxyapatite," *J. Mater. Sci. Lett.*, **17**, 381–3 (1998).

[25]E. Bertoni, A. Bigi, G. Falini, S. Panzavolta, and N. Roveri, "Hydroxyapatite/Polyacrylic Acid Nanocrystals," *J. Mater. Chem.*, **9** [3] 779–82 (1999).

[26]T. Iizuka and A. Nozuma, "Effects of the Buffer Solutions on the Growth of Hydroxyapatite Whiskers," *J. Ceram. Soc. Jpn.*, **107** [5] 442–8 (1999).

[27]T. Toyama, A. Oshima, and T. Yasue, "Hydrothermal Synthesis of Hydroxyapatite Whisker from Amorphous Calcium Phosphate and the Effect of Carboxylic Acid," *J. Ceram. Soc. Jpn.*, **109** [3] 232–7 (2001).

[28]K. Ioku, S. Yamauchi, H. Fujimori, S. Goto, and M. Yoshimura, "Hydrothermal Preparation of Fibrous Apatite and Apatite Sheet," *Solid State Ionics*, **151**, 147–50 (2002).

[29]D. Janackovic, I. Jankovic, R. Petrovic, L. Kostic-Gvozdenovic, S. Milonjic, and D. Uskokovic, "Surface Properties of HAP Particles Obtained by Hydrothermal Decomposition of Urea and Calcium-EDTA Chelates," *Key Eng. Mater.*, **240–242**, 437–40 (2003).

[30]J. Liu, X. Ye, H. Wang, M. Zhu, B. Wang, and H. Yan, "The Influence of pH and Temperature on the Morphology of Hydroxyapatite Synthesized by Hydrothermal Method," *Ceram. Int.*, **29**, 629–33 (2003).

[31]A. Mortier, J. Lemaitre, L. Rodrique, and P. G. Rouxhet, "Synthesis and Thermal Behavior of Well-Crystallized Calcium-Deficient Phosphate Apatite," *J. Solid State Chem.*, **78**, 215–9 (1989).

[32]M. Kinoshita, A. Kishioka, H. Hayashi, and K. Itatani, "Preparation of Fibrous Calcium Phosphates by Homogeneous Precipitation Method and their Thermal Changes," *Gypsum Lime*, **219**, 79–87 (1989).

[33]M. Kinoshita, K. Itatani, S. Nakamura, and A. Kishioka, "Preparation and Morphology of Carbonate-Containing Hydroxyapatite by Homogeneous Precipitation and Hydrothermal Methods," *Gypsum Lime*, **227**, 19–27 (1990).

[34]A. Barroug, J. Lemaitre, and P. G. Rouxhet, "Influence of Crystallite Size on the Surface Properties of Calcium-Deficient Hydroxyapatites," *J. Alloys Compds.*, **188**, 152–6 (1992).

[35]A. Yasukawa, H. Takase, K. Kandori, and T. Ishikawa, "Preparation of Calcium Hydroxyapatite Using Amides," *Polyhedron*, **13** [22] 3071–8 (1994).

[36]H. Zhang, Y. Wang, Y. Yan, and S. Li, "Precipitation of Biocompatible Hydroxyapatite Whiskers from Moderately Acid Solution," *Ceram. Int.*, **29**, 413–8 (2003).

[37]M. Aizawa, A. E. Porter, S. M. Best, and W. Bonfield, "Ultrastructural Observation of Single-Crystal Apatite Fibers," *Biomaterials*, **26** [1] 3427–33 (2005).

[38]D. Walsh, J. L. Kingston, B. R. Heywood, and S. Mann, "Influence of Monosaccharides and Related Molecules on the Morphology of Hydroxyapatite," *J. Cryst. Growth*, **133**, 1–12 (1993).

[39]K. Ishikawa, E. D. Eanes, and M. S. Tung, "The Effect of Supersaturation on Apatite Crystal Formation in Aqueous Solutions at Physiologic pH and Temperature," *J. Dent. Res.*, **73** [8] 1462–9 (1994).

[40]Y. Liu, G. Sethuraman, W. Wu, G. H. Nancollas, and M. Grynpas, "The Crystallization of Fluorapatite in the Presence of Hydroxyapatite Seeds and of Hydroxyapatite in the Presence of Fluorapatite Seeds," *J. Colloid Interface Sci.*, **186**, 102–9 (1997).

[41]T. Iizuka and A. Nozuma, "Effects of pH of the Aqueous Solutions on the Growth of Hydroxyapatite Whiskers," *J. Ceram. Soc. Jpn.*, **106** [8] 820–3 (1998).
[42]Y. Liu, W. Wang, Y. Zhan, C. Zheng, and G. Wang, "A Simple Route to Hydroxyapatite Nanofibers," *Mater. Lett.*, **56** [10] 496–501 (2002).
[43]R. Z. LeGeros, J. P. LeGeros, O. R. Trautz, and W. P. Shirra, "Conversion of Monetite, $CaHPO_4$, to Apatites: Effect of Carbonate on the Crystallinity and the Morphology of the Apatite Crystallites," *Adv. X-Ray Anal.*, **14**, 57–66 (1971).
[44]H. Monma, S. Ueno, and T. Kanazawa, "Properties of Hydroxyapatite Prepared by the Hydrolysis of Tricalcium Phosphate," *J. Chem. Technol. Biotechnol.*, **31**, 15–24 (1981).
[45]H. Monma and T. Kamiya, "Preparation of Hydroxyapatite by the Hydrolysis of Brushite," *J. Mater. Sci.*, **22**, 4247–50 (1987).
[46]K. Ioku, M. Yoshimura, and S. Somiya, "Hydrothermal Synthesis of Ultrafine Hydroxyapatite Single Crystals," *Nippon Kagaku Kaishi*, **9**, 1565–70 (1988).
[47]S. Somiya, K. Ioku, and M. Yoshimura, "Hydrothermal Synthesis and Characterization of Fine Apatite Crystals," *Mater. Sci. Forum*, **34–36**, 371–8 (1988).
[48]T. Hattori, Y. Iwadate, and T. Kato, "Hydrothermal Synthesis of Hydroxyapatite from Calcium Pyrophosphate," *J. Mater. Sci. Lett.*, **8**, 305–6 (1989).
[49]K. Ishikawa and E. D. Eanes, "The Hydrolysis of Anyhydrous Dicalcium Phosphate into Hydroxyapatite," *J. Dent. Res.*, **72** [2] 474–80 (1993).
[50]L. Yubao, K. de Groot, J. de Wijn, C. P. A. T. Klein, and S. V. D. Meer, "Morphology and Composition of Nanograde Calcium Phosphate Needle-Like Crystals Formed by Simple Hydrothermal Treatment," *J. Mater. Sci. Mater. Med.*, **5** [6–7] 326–31 (1994).
[51]L. Yubao, J. de Wijn, C. P. A. T. Klein, S. van de Meer, and K. de Groot, "Preparation and Characterization of Nanograde Osteoapatite-Like Rod Crystals," *J. Mater. Sci. Mater. Med.*, **5** [6–7] 252–5 (1994).
[52]A. Ito, S. Nakamura, H. Aoki, M. Akao, K. Teraoka, S. Tsutsumi, K. Onuma, and T. Tateishi, "Hydrothermal Growth of Carbonate-Containing Hydroxyapatite Single Crystals," *J. Cryst. Growth*, **163**, 311–7 (1996).
[53]K. Teraoka, A. Ito, K. Onuma, T. Tateishi, and S. Tsutsumi, "Hydrothermal Growth of Hydroxyapatite Single Crystals Under Natural Convection," *J. Mater. Res.*, **14** [6] 2655–61 (1999).
[54]A. Nakahira, K. Sakamoto, S. Yamaguchi, M. Kaneno, S. Takeda, and M. Okazaki, "Novel Synthesis Method of Hydroxyapatite Whiskers by Hydrolysis of α-Tricalcium Phosphate in Mixtures of Water and Organic Solvent," *J. Am. Ceram. Soc.*, **82** [8] 2029–32 (1999).
[55]A. Nakahira, K. Sakamoto, S. Yamaguchi, K. Kijima, and M. Okazaki, "Synthesis of Hydroxyapatite by Hydrolysis of α-TCP," *J. Ceram. Soc. Jpn.*, **107** [1] 89–91 (1999).
[56]H. Katsuki, S. Furuta, and S. Komarneni, "Microwave-Versus Conventional-Hydrothermal Synthesis of Hydroxyapatite Crystals from Gypsum," *J. Am. Ceram. Soc.*, **82** [8] 2257–9 (1999).
[57]G. C. Koumoulidis, T. C. Vaimakis, A. T. Sdoukos, N. K. Boukos, and C. C. Trapalis, "Preparation of Hydroxyapatite Lathlike Particles Using High-Speed Dispersing Equipment," *J. Am. Ceram. Soc.*, **84** [6] 1203–8 (2001).
[58]R. E. Riman, W. L. Suchanek, K. Byrappa, C-W. Chen, P. Shuk, and C. S. Oakes, "Solution Synthesis of Hydrothermal Designer Particulates," *Solid State Ionics*, **151**, 393–402 (2002).
[59]K. Ioku, M. Toda, H. Fujimori, S. Goto, and M. Yoshimura, "Hydrothermal Preparation of Granular Hydroxyapatite with Controlled Surface," *Key Eng. Mater.*, **254–256**, 19–22 (2004).
[60]H. C. Park, D. J. Baek, Y. M. Park, S. Y. Yoon, and R. Stevens, "Thermal Stability of Hydroxyapatite Whiskers by Derived from the Hydrolysis of α-TCP," *J. Mater. Sci.*, **39**, 2531–4 (2004).
[61]S. Y. Yoon, Y. M. Park, S. S. Park, R. Stevens, and H. C. Park, "Synthesis of Hydroxyapatite Whiskers by Hydrolysis of α-Tricalcium Phosphate Using Microwave Heating," *Mater. Chem. Phys.*, **91**, 48–53 (2005).
[62]Y. Ota, T. Iwashita, T. Kasuga, and Y. Abe, "Novel Preparation Method of Hydroxyapatite Fibers," *J. Am. Ceram. Soc.*, **81** [6] 1665–8 (1998).
[63]A. C. Tas, "Molten Salt Synthesis of Calcium Hydroxyapatite Whiskers," *J. Am. Ceram. Soc.*, **84** [2] 295–300 (2001).
[64]S. Jalota, A. C. Tas, and S. B. Bhaduri, "Microwave-Assisted Synthesis of Calcium Phosphate Nanowhiskers," *J. Mater. Res.*, **19** [6] 1876–81 (2004).
[65]J. C. Elliott, *Structure and Chemistry of the Apatites and Other Calcium Orthophosphates*. Elsevier Science B.V., Amsterdam, The Netherlands, 1994.
[66]N. Balmain, R. Legros, and G. Bonel, "X-Ray Diffraction of Calcined Bone Tissue: A Reliable Method for the Determination of Bone Ca/P Molar Ratio," *Calcif. Tissue Int.*, **34**, S93–S98 (1982).
[67]K. Ishikawa, P. Ducheyne, and S. Radin, "Determination of the Ca/P Ratio in Calcium-Deficient Hydroxyapatite Using X-Ray Diffraction Analysis," *J. Mater. Sci. Mater. Med.*, **4**, 165–8 (1993).
[68]S. Raynaud, E. Champion, D. Bernache-Assollant, and J.-P. Laval, "Determination of Calcium/Phosphorus Atomic Ratio of Calcium Phosphate Apatites Using X-Ray Diffractometry," *J. Am. Ceram. Soc.*, **84** [2] 359–66 (2001).
[69]B. O. Fowler, E. C. Moreno, and W. E. Brown, "Infra-Red Spectra of Hydroxyapatite, Octacalcium Phosphate and Pyrolysed Octacalcium Phosphate," *Arch. Oral Biol.*, **11**, 477–92 (1966).
[70]B. O. Fowler, "Infrared Studies of Apatites. I. Vibrational Assignments for Calcium, Strontium, and Barium Hydroxyapatites Utilizing Isotopic Substitution," *Inorg. Chem.*, **13** [1] 194–207 (1974).
[71]B. R. Heywood, N. H. C. Sparks, R. P. Shellis, S. Weiner, and S. Mann, "Ultrastructure, Morphology and Crystal Growth of Biogenic and Synthetic Apatites," *Conn. Tissue Res.*, **25** [2] 103–19 (1990).
[72]J. Moradian-Oldak, S. Weiner, L. Addadi, W. J. Landis, and W. Traub, "Electron Imaging and Diffraction Study of Individual Crystals of Bone, Mineralized Tendon and Synthetic Carbonate Apatite," *Conn. Tissue Res.*, **30** [3–4] 219–28 (1991).
[73]K. Sato, T. Kogure, Y. Kumagai, and J. Tanaka, "Crystal Orientation of Hydroxyapatite Induced by Ordered Carboxyl Groups," *J. Colloid Interface Sci.*, **240**, 133–8 (2001).
[74]G. H. Nancollas and P. G. Koutsoukos, "Calcium Phosphate Nucleation and Growth in Solution," *Prog. Cryst. Growth Charact.*, **3**, 77–102 (1980).
[75]A. E. Martell and R. M. Smith, *Critical Stability Constants, Volume 3: Other Organic Ligands*. Plenum Press, New York, NY, 1977.
[76]S. P. Chahal, "Lactic Acid"; pp. 97–105 in *Ullmann's Encyclopedia of Industrial Chemistry*, 5th Edition, Vol. A15, Edited by B. Elvers, S. Hawkins, and G. Schulz. VCH, Weinheim, 1990.
[77]Cosmetic Ingredient Review Expert Panel. Final Report on the Safety of Assessment of Glycolic Acid, Ammonium, Calcium, Potassium, and Sodium Glycolates, Methyl, Ethyl, Propyl, and Butyl Glycolates, and Lactic Acid, Ammonium, Calcium, Potassium, Sodium, and Tea-Lactates, Methyl, Ethyl, Isopropyl, and Butyl Lactates, and Lauryl, Myristyl, and Cetyl Lactates," *Int. J. Toxic.*, **17** [Suppl. 1] 5–25 (1998).
[78]A. E. Martell and R. D. Hancock, *Metal Complexes in Aqueous Solutions*. Plenum Press, New York, NY, 1996.
[79]M. M. Lencka and R. E. Riman, "Thermodynamics of the Hydrothermal Synthesis of Calcium Titanate with Reference to Other Alkaline-Earth Titanates," *Chem. Mater.*, **7** [1] 18–25 (1995).
[80]M. J. Glimcher, L. C. Bonar, M. D. Grynpas, W. J. Landis, and A. H. Roufosse, "Recent Studies of Bone Mineral: Is the Amorphous Calcium Phosphate Theory Valid?" *J. Cryst. Growth*, **53**, 100–19 (1981).
[81]E. C. Moreno and K. Varughese, "Crystal Growth of Calcium Apatites from Dilute Solutions," *J. Cryst. Growth*, **53**, 20–30 (1981).
[82]H. Furedi-Milhofer, J. Moradian-Oldak, S. Weiner, A. Veis, K. P. Mintz, and L. Addadi, "Interactions of Matrix Proteins from Mineralized Tissues with Octacalcium Phosphate," *Conn. Tissue Res.*, **30**, 251–64 (1994).
[83]K. Sato, Y. Suetsugu, J. Tanaka, S. Ina, and H. Monma, "The Surface Structure of Hydroxyapatite Single Crystal and the Accumulation of Arachidic Acid," *J. Colloid Interface Sci.*, **224**, 23–7 (2000).
[84]K. Flade, C. Lau, M. Mertig, and W. Pompe, "Osteocalcin-Controlled Dissolution-Reprecipitation of Calcium Phosphate Under Biomimetic Conditions," *Chem. Mater.*, **13** [10] 3596–602 (2001). □